# ACS Energy LETTERS

Electronic Traps and Phase Segregation in Lead Mixed-Halide Perovskite

Alexander J. Knight, Adam D. Wright, Jay B. Patel, David P. McMeekin, Henry J. Snaith, Michael B. Johnston, and Laura M. Herz*

Department of Physics, University of Oxford, Clarendon Laboratory, Parks Road, Oxford OX1 3PJ, United Kingdom

S Supporting Information

ABSTRACT: An understanding of the factors driving halide segregation in lead mixed-halide perovskites is required for their implementation in tandem solar cells with existing silicon technology. Here we report that the halide segregation dynamics observed in the photoluminescence from $CH_3NH_3Pb(Br_{0.5}I_{0.5})_3$ is strongly influenced by the atmospheric environment, and that encapsulation of films with a layer of poly(methyl methacrylate) allows for halide segregation dynamics to be fully reversible and repeatable. We further establish an empirical model directly linking the amount of halide segregation observed in the photoluminescence to the fraction of charge carriers recombining through trap-mediated channels, and the photon flux absorbed. From such quantitative analysis we show that under pulsed illumination, the frequency of the modulation alone has no influence on the segregation dynamics. Additionally, we extrapolate that working $CH_3NH_3Pb(Br_{0.5}I_{0.5})_3$ perovskite cells would require a reduction of the trap-related charge carrier recombination rate to $\lesssim 10^5 s^{-1}$ in order for halide segregation to be sufficiently suppressed.
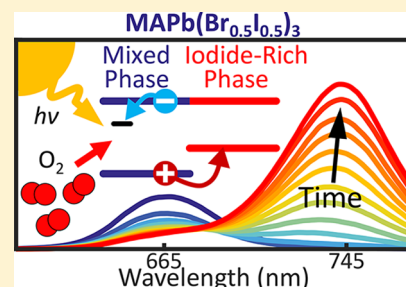
The rapid rise in performance of metal halide perovskite photovoltaic devices over recent years has strengthened the prospects for commercial exploration of this technology.[1,2] However, the current market dominance of silicon solar cells[3] and their high power conversion efficiencies make direct competition challenging. One promising avenue is therefore the augmentation of existing silicon cells with perovskite thin films to form perovskite−silicon tandems,[4−7] which would allow manufacturers to partially circumvent the thermodynamic losses inherent to single-junction cells[8] and thus inexpensively increase overall cell efficiencies.

Highly efficient two-terminal tandem solar cells rely on the careful choice of bandgaps for the composite layers in order for the cell to extract maximum energy from the solar spectrum. Currently, the most promising hybrid perovskites for two-terminal cells are based on lead iodide−bromide perovskites (stoichiometry $APb(Br_xI_{1-x})_3$, where A is a monovalent cation, typically $CH_3NH_3^+$, $CH(NH_2)_2^+$, Cs^+, or a mixture thereof) whose bandgap can be tuned through the ratio of the two halide ions.[4,9−12] Unfortunately, photoluminescence (PL) techniques have revealed that the bandgap of these materials typically red shifts under illumination,[10,13] an undesirable trait in particular for a tandem solar cell material.[14−16] This bandgap shift has been attributed to spatial segregation of the different halide ions in the perovskite,[13] resulting in separated regions of iodide-rich and bromide-rich perovskites within the remaining well-mixed phase. Charge carriers funnel and recombine in the new lowest-energy states—those within the iodide-rich phase—creating the observed red shift of emitted light. It has been reported that, bizarrely, once the incident illumination is turned off, the perovskite gradually returns to its initial well-mixed state, with further segregation and remixing then inducible with illumination and darkness, respectively.[13] Reports have shown that halide segregation is dependent on the perovskite film morphology, with improved material crystallinity correlated with reduced amounts of segregation.[17−19] Halide segregation has also been observed in the absence of light, when charge carriers are injected into the film via an electric potential difference,[14,16] and extraction of excited charge carriers from the perovskite film was found to lower the extent of segregation.[16] These observations imply that the existence of excited charge carriers in the material plays a prominent role in the halide segregation process; however, a consensus in the literature has yet to be reached on the full underlying mechanisms.

In addition, there is vast and varied literature on the changes observed in the optoelectronic properties of single-halide perovskites under different atmospheres.[20−28] Reports have shown that under light soaking an oxygen-rich environment increases the photoluminescence quantum yield (PLQY) of $MAPbI_3$[20−26] and $MAPbBr_3$[27,28] films (MA = $CH_3NH_3^+$), which has been attributed to a decrease in the density of electronic trap states. However, Quitsch et al. observed both photobrightening and photodarkening of $MAPbI_3$ films
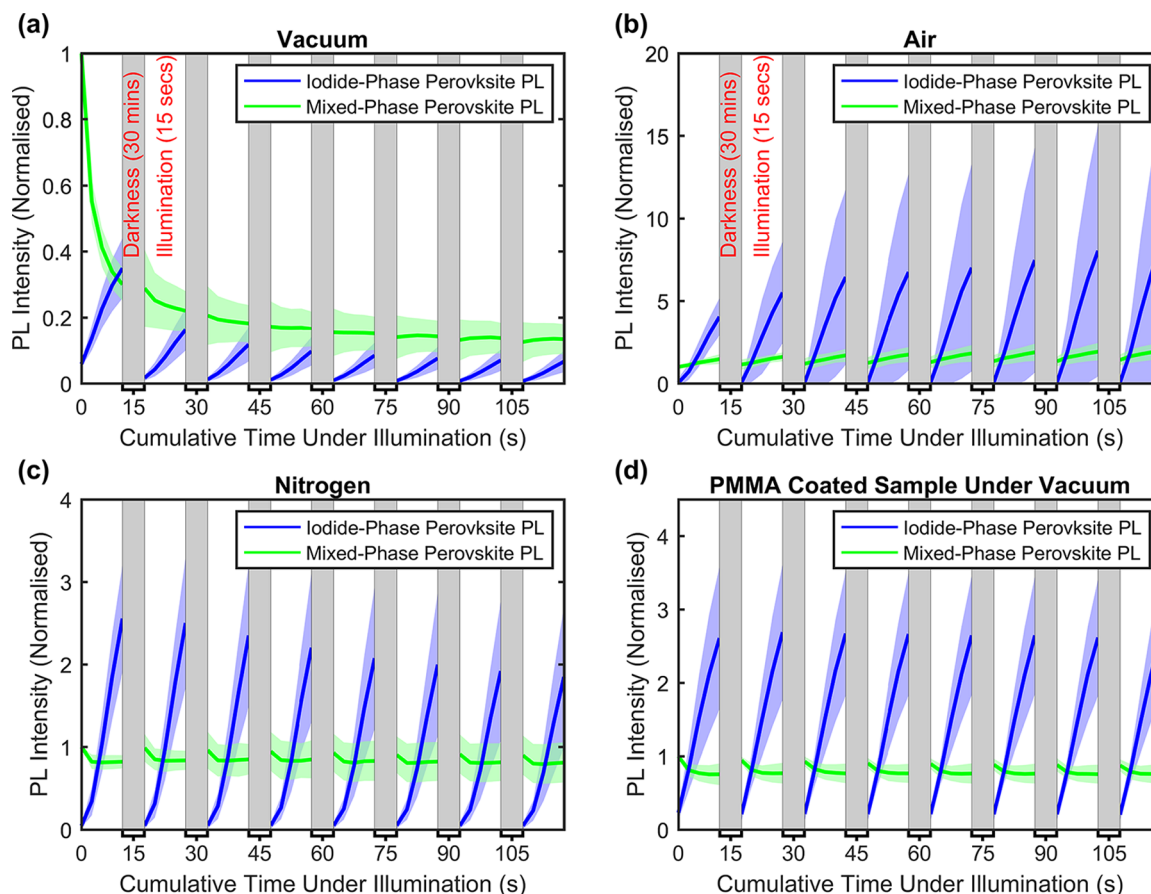
Figure 1. Evolution of PL emission monitoring the reversibility of halide segregation when $MAPb(Br_{0.5}I_{0.5})_3$ films are held under four different atmospheric conditions, (a) under vacuum (~0.2 mbar), (b) ambient air, (c) pressurized (2 bar) nitrogen, and (d) film topped with a layer of PMMA and held under vacuum (~0.2 mbar). To induce repeated segregation and remixing, the films were exposed to eight illumination cycles, with a single cycle consisting of 15 s of illumination followed by 30 min of darkness. Illumination was achieved with a laser of wavelength 400 nm whose intensity was adjusted to provide excitation equivalent to AM1.5 solar illumination (see SI section S3). The bold blue lines show the mean integrated intensity of the PL originating from the iodide-rich phase (720−770 nm), while the bold green lines give the mean integrated intensity of the PL from the mixed-halide (640−690 nm), both scaled such that the initial mixed-halide PL intensity is set to 1. Bold lines are the calculated mean over several repeats of such runs on fresh areas of perovskite film (shown in section S4 of the SI), and shaded regions indicate the values within one standard deviation of the mean, thus highlighting the extent of spot-to-spot variations.

depending on the wavelength of the illumination source,[25] and Tian et al. found vastly different types of behavior even for different grains of the same MAPbI$_3$ film.[21] Humidity has also been reported to cause photobrightening in the short term;[20,24,27] however, over longer time frames both oxygen and humidity have been shown to individually cause degradation of perovskite films.[29−32] Under vacuum, a decrease in the PL signal upon light soaking is generally reported,[20,28,33] and under nitrogen, smaller changes are observed, which may carry signs of either photobrightening[23] or photodarkening.[20]

To explain the observed changes under oxygen, it has been proposed that oxygen molecules diffuse into the perovskite crystal and react with photogenerated charge carriers[20,21] to form a superoxide species (O_2^-), which is then well suited in its charge and size to fill iodide vacancies, thus passivating potential trap states.[20,22,24,28] Alternatively, PbI$_2$ has also been suggested as the trap-passivating species,[26,34] with photobrightening observed under a humid atmosphere[20,24] attributed to the benign effects of PbI$_2$ formation.

These observations open the interesting question of whether the atmospheric effects that change the PLQE of perovskite films also influence the underlying dynamics of halide segregation. As the movement of halide ions through the film is thought to occur through lattice-site hopping,[35] a superoxide species residing in halide vacancy sites should decrease the halide ion mobility, which would then decrease the rate of halide segregation. As halide ions travel much faster along grain boundaries,[36−38] the formation of PbI$_2$ in these regions should also affect the rate of halide segregation. Furthermore, we show in this work that excited charge carriers that recombine through trap states influence the speed of halide segregation. Thus, any mechanism that changes the density of trap states should alter the segregation dynamics and the associated changes observed in the PL spectra.

Given the potential of mixed-halide perovskites as tandem solar cell materials, a detailed understanding of the underlying mechanisms behind these atmosphere-caused changes and halide segregation is desired, with the ultimate aim of suppression or exploitation of these mechanisms under working conditions. Unfortunately, the segregation dynamics reported from PL experiments in the literature are often inconsistent; even among similar perovskite compositions and illumination intensities, the time taken for halide ions to

segregate varies between tens of seconds[13,39,40] and tens of minutes,[4,41,42] and the intensity ratio of the initial and final PL peaks varies between roughly 2 and more than 6.[4,13,39−42] In addition, the role of crystallinity in halide segregation[17−19,39] and the role of excess halide ions in halide segregation[42,43] have been debated. We note that in these and other[12,44,45] reports the PL measurements were conducted with the samples held in either nitrogen, in air, under vacuum, or in an unspecified atmosphere. Given the changes in PL intensities that are known to be induced by light in single-halide perovskites over time, such discrepancies in the literature may therefore potentially be caused by the differences in the atmosphere under which perovskites were held.

In this work, we resolve the contradictions in the literature by carefully examining the role of the environmental atmosphere on halide segregation dynamics in MAPb-$(Br_{0.5}I_{0.5})_3$ observed through PL experiments. We find that changes in the PL spectra of mixed-halide perovskites under illumination vary markedly under different atmospheres, with overall trends in PL amplitudes resembling changes observed in single-halide perovskites, which are however combined with environmentally dependent halide segregation dynamics. We demonstrate that the influence of atmospheric changes can be mostly suppressed by encapsulation of the perovskite films with a thick (>1 μm) layer of poly(methyl methacrylate) (PMMA), which allows for an examination of the role of photogenerated charge carrier density on the dynamics of halide segregation. We show that charge carriers recombining through trap-mediated routes are responsible for halide segregation, which allows us to create an empirical model for the growth of iodide-rich perovskite PL over time, as a function of various film and illumination parameters. From such considerations, we are able to predict that a reduction of the trap-related charge carrier recombination rate to $\lesssim 10^5$ s^{-1} (τ_{PL} $\gtrsim 5$ μs) would be sufficient for halide segregation to be largely suppressed in working perovskite solar cells based on MAPb$(Br_{0.5}I_{0.5})_3$. As a reference point, we estimate the trap-related charge carrier recombination rate to be $\sim 5 \times 10^6$ s^{-1} in the MAPb$(Br_{0.5}I_{0.5})_3$ films that we study here (see section 8 of the SI). We are further able to reveal that if modulated light is used to photoexcite mixed-halide perovskites, the frequency of the modulation alone has no influence on the segregation dynamics. Finally, we conclude that light-induced halide segregation can be understood as a positive feedback system, initiated by electric fields arising from trapped charge carriers and further driven by funneling of charge carriers into the generated lower-energy iodide-rich domains.

We begin our study by establishing how atmospheric conditions influence the changes observed in the PL spectrum of mixed-halide perovskite films during halide segregation and remixing experiments. Assessment of such environmental factors is not only useful for research laboratory studies but will also give insight into the operation of these wide-bandgap materials under real-world conditions. Figure 1 shows that under illumination, the PL spectra of a MAPb$(Br_{0.5}I_{0.5})_3$ perovskite film exhibit a complex fingerprint of both halide segregation and atmospheric effects. Here, the 390 nm thick films were periodically exposed to light under different atmospheric conditions for eight cycles of induced halide segregation and remixing, where each cycle consisted of 15 s of illumination, followed by 30 min of darkness. Illumination was conducted by a laser of 400 nm wavelength at AM1.5 equivalent intensity (see SI section S3 for details). Four

different atmospheric conditions were explored: vacuum (around 0.2 mbar), air, pressurized nitrogen (around 2 bar), and vacuum with a PMMA top-coating to encapsulate the perovskite films. In order to allow us to probe the full range of segregation and remixing dynamics, the periods of darkness were 120 times as long as the periods of illumination to ensure that the films had sufficient time to recover from the halide segregation. The graphs in Figure 1 show two integrated intensities from the perovskite PL spectrum (see Figure S4); a range of 720−770 nm is plotted in blue and follows the iodide-rich perovskite PL peak, and a range of 640−690 nm is plotted in green and follows the mixed-phase PL peak, both scaled such that the initial mixed-phase PL measurement is set to 1. In order for us to account for spot-to-spot variations in the perovskite, several repeats under each atmospheric condition were performed on different areas of the films. The bold lines in Figure 1 show the averaged data from these repeats, and the shaded regions indicate values within one standard deviation of the mean.

Each light/dark cycle for any of the four atmospheric conditions clearly displays an increase in the PL signal of the iodide-rich phase under illumination, indicating that lower-bandgap, iodide-rich perovskite regions are forming within the remaining well-mixed phase. The growth rate of the low-bandgap signal is heavily dependent on the surrounding atmosphere, with different maximum PL signal intensities reached under the different atmospheres, despite identical illumination conditions used. As the low-bandgap signal was found to have returned to its initial value at the start of every repeat cycle, we conclude that the 30 min of darkness within each cycle was sufficient to allow the segregated perovskite to remix. However, under vacuum and under air, the films otherwise clearly do not fully revert to their initial states under darkness, given that the halide segregation dynamics recorded in subsequent cycles progressively differ from those observed in the first cycle. Comparing PL amplitudes from either the iodide-rich or mixed-phase peaks across similar points in each cycle (e.g., the last point of each cycle), we find that the long-term changes in the PL intensities displayed in Figure 1 are qualitatively similar to those reported for single-halide perovskites under comparable conditions. For such single-halide perovskites, the PL has been found to decrease under vacuum,[20,28,33] increase in air,[20−28] and remain fairly constant under nitrogen,[20,23,27] similar to what we observe here for the average PL signal of MAPb$(Br_{0.5}I_{0.5})_3$ across cycles. Similarly, the large standard deviation we observe in the halide segregation dynamics for the mixed-halide samples held under air is reminiscent of the diverse PL changes reported in the literature for single-halide perovskites under illumination in air.[21] Such variations under air likely result from a combination of slight differences in the atmospheric composition, perovskite film inhomogeneity, the degree the perovskite contacts the atmosphere, and the fact that oxygen and water undergo complex chemical processes with the perovskite.[29−31] Importantly, we note that when MAPb-$(Br_{0.5}I_{0.5})_3$ films are coated with PMMA, the changes observed in the PL spectra under illumination in vacuum are highly repeatable between cycles (Figure 1d). Under air and nitrogen, such PMMA coating also yielded a suppression of atmospheric effects (see SI section S4), although it was not as complete as that under vacuum.

Given these observations, we suggest that the proposed photoinduced processes that moderate charge carrier traps in

single-halide perovskites under different atmospheres also occur within mixed-halide perovskites: under vacuum, the average PL signal across cycles is reduced as the number of electronic trap states in the perovskite film increases,[20,28] and under air, the formation of a superoxide species passivates trap states and increases the average PL signal across cycles.[20−22,24] Under nitrogen or under vacuum with a PMMA coating protecting the films, on the other hand, neither the photobrightening nor the photodarkening process may occur.[20] These differences in electronic trap densities or efficacies may affect both the quantum efficiency of PL and the dynamics of halide segregation, leading to the large atmospheric variation in the curves displayed in Figure 1.

Our observations also highlight that while halide segregation is reversible under certain atmospheric conditions, under vacuum or air, photoinduced changes occur that cannot be reversed under darkness. This irreversibility is an important issue as many measurements of halide segregation reported in the literature are not concerned with the remixing process in the dark but rather record halide segregation over one cycle only.[4,12,17−19,39−41,44,45] However, it is apparent from Figure 1 that the atmospheric conditions under which halide segregation measurement is made will alter the dynamics observed. The difference in observed dynamics will be amplified if the perovskite is assumed to have recovered between measurements and measurements are then taken from the same area of the film. Thus, we suggest that comparisons of data in the existing literature must be done with care.

In addition, our findings elucidate the extent to which halide segregation will be reversible under real-world operating conditions for photovoltaic cells. As Figure 1d shows, the atmosphere-induced changes to the perovskite film can be prevented with a thick protective coating of PMMA. In working perovskite solar cells, the electrical contacts and charge carrier transport materials could most likely provide similar protection, and an additional encapsulation will most likely also be present. Therefore, halide segregation would most likely be fully reversible in commercial solar cell modules, although still clearly undesirable because of the associated voltage losses. In order to exclude atmospheric effects and focus on a scenario relevant to PV operation, we performed the remaining work in this study on PMMA-coated MAPb-(Br$_{0.5}$I$_{0.5}$)$_3$ films held under vacuum.

Despite the large volume of literature[10,12−19,33,39−50] on halide segregation in mixed-halide perovskites, there is yet to be a definitive explanation of the underlying mechanisms that drive the different halide ions apart in the presence of light. There is evidence that excited charge carriers are responsible,[14,16] but little is known about how these free charge carriers drive halide segregation. In order to probe how the density of charge carriers affects halide segregation, we illuminated perovskite films with a constant number of total photons over different lengths of time, thus changing the generation rate of free charge carriers. Keeping the total incident photon number constant meant, for example, halving the illumination laser intensity if the exposure time was doubled. We found that a subset of the photoexcited charge carriers—those that recombine through electronic trap states—determine the rate of halide segregation. This result provides further insight into the segregation mechanism and allows us to present a possible model for the observed halide segregation dynamics.

Figure 2a shows how the growth of the PL signal from the iodide-rich perovskite (taken as the spectral integral between
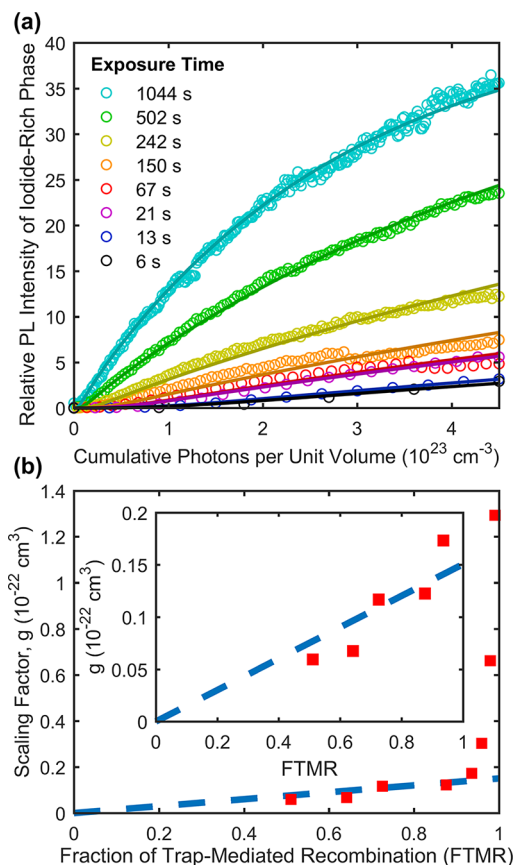

Figure 2. (a) Evolution of the PL intensity originating from the low-bandgap iodide-rich phase of MAPb(Br$_{0.5}$I$_{0.5}$)$_3$ plotted against the number of incident photons per unit volume for different overall exposure times to illumination but constant total incident photons. The hoops represent experimental data points, and the solid lines are the fits of eq 1 to the data: see SI section S5 for additional experimental details. (b) Evolution of the fitting parameter g with an increasing fraction of trap-mediated recombination, taken from the fits of eq 1 to the data in (a). The first five points exhibit a linear relationship, fitted by the dashed blue line with a gradient of 1.5×10^{-23} cm^3, which is followed by a sharp onset in g. The inset shows a scaled view of the first five data points. The dashed lines are expected to pass through the origin because halide segregation is assumed to be absent when there is no charge carrier trapping or illumination.

720 and 770 nm) depends on the illumination exposure time and thus the photoexcited charge carrier generation rate. The PL intensity from the iodide-rich phase was normalized such that the initial integrated intensity of the mixed-phase peak (taken as the spectral integral between 640 and 690 nm) was set to 1, in order to provide a measure of halide segregation in terms of the relative peak amplitudes, independent of the different illumination powers used. These normalized PL intensities for each exposure time were then plotted against the cumulative number of photons incident per unit volume on the perovskite film. In each case, the low-bandgap PL signal starts at zero intensity (when the perovskite is well mixed) and then increases as the iodide-rich perovskite phase forms. In order to avoid spot-to-spot differences, following illumination the films were left in the dark so that the halides would remix for around

45 min before the next exposure time experiment was performed on exactly the same area of the film.

The graphs presented in Figure 2a are particularly interesting because they reveal that as the illumination exposure time is increased an increasing level of halide segregation is encountered even when the same number of cumulative photons has been incident on the film. In other words, if halide segregation only depended on the accumulated number of photoexcited charge carriers generated, then there should be no difference between our experimental runs at points where the same total photon input has been incident, which is clearly not the case. For experiments with longer exposure time, the illumination intensity is lower, photo-exciting a smaller charge carrier density within the perovskite film. Therefore, the efficacy of a charge carrier to induce halide segregation (per unit carrier) appears higher at lower charge carrier density. These observations can be understood if one considers the changing contributions of various charge carrier recombination processes in metal halide perovskites as the charge carrier density is increased.[51] While at low carrier densities, monomolecular, trap-mediated charge recombination dominates, radiative bimolecular band-to-band recombination becomes increasingly dominant at higher densities (see section S6 in the SI for detailed calculations). Thus, our data support the conclusion that excited charge carriers that recombine through trap states mediate halide segregation as we observe more segregation per photon at longer exposure time when lower charge densities lead to larger proportions of the excited charge carriers being trapped.

Further examination of the segregation dynamics reveals that the overall temporal evolution of the iodide-rich phase signal is extremely similar across all exposure times, i.e., the shapes of the curves are alike, with only the extent reached along the path dictated by the exposure time. In Figures S14 and S15 in the SI, we show that the traces displayed in Figure 2a can be superimposed on each other by a suitably chosen x-axis scaling for each curve. Mathematically, this indicates that a single global function will provide an accurate fit to all of the experimental runs, with only one local fitting parameter required to scale the x-axis to account for the different exposure times. We find that the following function empirically describes the intensity $I_{\text{(I-rich PL)}}$ of the PL originating from the iodide-rich phase in the perovskite accurately as a function of incident photons per unit volume

$$I_{\text{(I-rich PL)}} = f(gGt) = A\frac{(gGt)^2}{(1 + (gGt)^2)}(1 - e^{-BgGt}) \qquad (1)$$

Here G is the generation rate of excited charge carriers per unit volume measured in cm^{-3} s^{-1}, t is time, A is a dimensionless global fitting parameter that is dependent on the exact method used to define $I_{\text{(I-rich PL)}}$ and measured to be 43.6 for our setup (see SI section S5 for more details), B is a dimensionless global parameter determined from fits to be 27.5×10^{-3}, and g is the local fitting parameter that represents the scaling of the x-axis, given in centimeters cubed. The functional form of eq 1 incorporates two main features that we observe in the data, which are that halide segregation appears to have a delayed onset, i.e., it shows an initially very flat/shallow rise whose gradient then accelerates and that the segregation slows and saturates at long exposure times. The delayed onset is captured by the first factor (the fraction) in eq 1, while the latter rise is represented by the second factor that reflects growth through

an exponential asymptote with characteristic rise constant B. The final relative segregation attained is reflected by the expression tending to the value of A at long times. We note that a purely exponential form has previously been used to empirically fit the rise in the PL amplitude of the iodide-rich phase as the perovskite segregates,[39] but we find that this did not adequately capture the initial slow rise of signal especially visible at low exposure times, as highlighted in Figure S15.

The fact that our data can be captured by a global function indicates that the underlying, intrinsic halide segregation dynamics rely on a single dominating mechanistic pathway, with the local scaling factor, g, providing a measure of the differing degrees of segregation in a unit volume caused per excited charge carrier at different illumination intensities. g can thus be thought of as a charge carrier efficacy for inducing halide segregation.

Increased exposure time serves to increase the proportion of charge carriers that recombine through trap states, which is shown in Figure 2a to be correlated with an increase in the amount of halide segregation caused per incident photon per unit volume. As excited charge carriers, rather than photons, have been shown to be an essential component driving the halide segregation mechanism,[14,16] we therefore wish to determine the dependence of g on the fraction of charge carriers that recombine through trap states. By determining the generation rate of excited charge carriers from the exposure time and considering the relevant recombination constants for trap-mediated, bimolecular, and Auger recombination processes, we are able to determine the fractions for trap-mediated charge carrier decay in our measurements, as described in detail in SI section S6. Figure 2b then displays the scaling factor g (extracted from fits shown in Figure 2a) as a function of the trap-mediated charge decay fraction. At low fractions of trap-mediated recombination (less than around 95%), Figure 2b displays a linear region (highlighted by the inset), possibly suggesting that the underlying halide segregation mechanisms depend linearly on the fraction of charge carriers that recombine through trap states in the perovskite films. This linear increase of g with the fraction of trapped charges reflects the increased efficacy of charge carriers for inducing halide segregation at longer exposure times, for which charge carrier densities are reduced in our experiments (constant overall photon dose). At higher fractions of trap-mediated recombination, there is a sharp onset in g, which we suggest is a result of the longer exposure times used in these experimental runs allowing for greater movement of the halide ions despite saturation of the fraction of trap-mediated recombination. This conclusion is supported by Figure S16 in the SI, which plots g against experimental exposure time and displays a linear region for the longest three exposure times (corresponding to the three data points within the sharp onset in g in Figure 2b), suggesting that within this region the halide segregation mechanics become dominated by the time the sample is under illumination.

The phenomenological parametrization of halide segregation through eq 1 is highly useful as it allows for predictions to be made on the extent of halide segregation under various circumstances. As we show in detail below, such knowledge then allows, for example, an understanding of the recently observed[46] apparent dependence of halide segregation on excitation pulse frequency and assessment of the degree to which trap-related charge recombination has to be suppressed in order for halide segregation to become insignificant under

PV operation conditions. Equation 1 depends on four parameters, A, B, G, and g, and one variable t, time. A and B both depend on the exact perovskite material excited under illumination, and A further depends on the definition used for the iodide-rich and mixed-phase PL peaks. For our experimental setup and perovskite films, we determined A and B to have dimensionless values of 43.6 and 27.5×10^{-3}, respectively, which is assumed to be similar to the values of A and B for equivalent PL experiments performed on similar perovskite films. The charge carrier generation rate per unit volume, G, is calculated from knowledge of the illumination source and film thickness, and the charge carrier efficacy, g, is derived from its fitted, linear dependence on the fraction of charge carriers that recombine via trap states, as shown in Figure 2b. The fraction of trap-related charge recombination can itself be calculated from the illumination and recombination rate parameters (see SI section S6). Once A, B, G, and g are known, eq 1 determines the relative strength of the iodide-rich PL, which is related to the degree of phase segregation the perovskite film has experienced. We note that while the form of the empirical function in eq 1 is expected to be inherent to perovskite films that undergo halide segregation, the values of A, B, and g may vary with composition (iodide:bromide ratio) and temperature. For the $MAPb(Br_{0.5}I_{0.5})_3$ perovskite under investigation at room temperature here, Figure 3 shows the
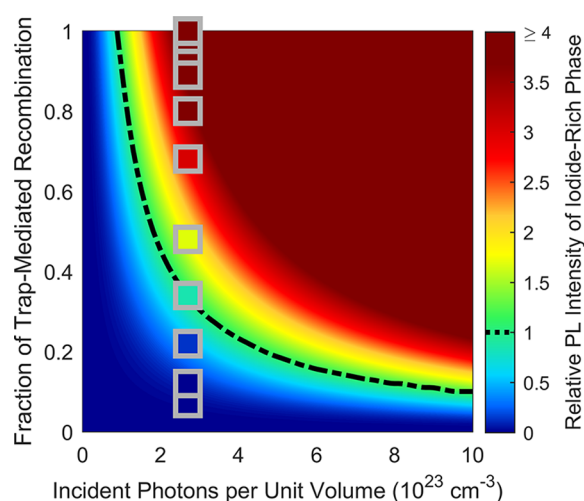

Figure 3. Color map showing the predicted relative PL intensity originating from the iodide-rich phase of a $MAPb(Br_{0.5}I_{0.5})_3$ film, as a function of both the fraction of charge carriers recombining through traps and the number of photons incident on the film per unit volume $(G \times t)$. The PL intensity is normalized such that 1 corresponds to the intensity of the mixed-halide PL in the absence of segregation and under similar illumination conditions. The black, dashed line indicates the points at which the PL peak of the iodide-rich phase begins to dominate the spectrum. The gray bordered squares represent halide segregation experiments performed by Yang et al. for which the average power of a pulsed illumination source was kept constant while the repetition rate of the laser pulses was varied.[46] The interior color of the squares roughly indicates the relative level of iodide-rich perovskite PL observed, which, together with other parameters, was extracted from the work of Yang et al., as described in section S7 of the SI. The good agreement of colors inside of the squares with that in their vicinity shows that the variation in repetition rate in these experiments only affects halide segregation because it also changes the fraction of charge carriers recombining through traps.

resulting color plot representing the amount of segregation expected when the fraction of carriers undertaking trap-mediated recombination or the number density of cumulative photons incident on the perovskite is varied. The map graphically illustrates how the degree of segregation a perovskite film experiences increases with the number of incident photons and/or fraction of charge carriers that recombine via trap states.

Interestingly, our findings allow us to resolve the reasons for an apparent dependence of halide segregation on the pulse repetition frequency of excitation that had recently been observed. Yang et al. reported that under pulsed laser illumination at fixed average power, the degree of halide segregation observed in a $MAPb(Br_{0.57}I_{0.43})_3$ perovskite film was dependent on the repetition rate of the laser pulses.[46] They observed that no significant halide segregation occurred below a pulse frequency of 500 Hz over the course of 10 min, whereas above this repetition rate they found an increasing dominance of an iodide-rich perovskite peak in the PL spectrum when the average intensity and time of the illumination were kept constant. We believe that their observations can be explained by our model as, in order to fix the average power to a constant value while changing the laser pulse repetition rate, Yang et al. correspondingly changed the instantaneous excitation pulse intensity, which would have altered the initially injected charge carrier density in the film. For example, a decreased repetition rate would require a higher pulse fluence (higher instantaneous intensity) to maintain the same fixed average intensity value, which would increase the charge carrier density injected with each pulse, thus enhancing the radiative band-to-band recombination rate and lowering the fraction of charge carriers that recombine through trap states.

The apparent frequency dependence observed in the study by Yang et al. is therefore an indirect effect, resulting from changes in charge-trapping with injected charge carrier density, and we would not expect a direct link between halide segregation and light modulation frequency. To prove this point experimentally, we performed a halide segregation experiment during which $MAPb(Br_{0.5}I_{0.5})_3$ films were exposed to light modulated by a square-wave ("on−off") function of 50% duty cycle and variable frequency (see the inset in Figure 4). Unlike in the study by Yang et al.[46] we therefore here kept both the pulse intensity *and* the overall intensity constant as the frequency was changed, i.e., the variation in frequency was accomplished by a mere change in the width of each square-wave pulse (see Figure S18 in the SI for a comparison sketch of the two different illumination scenarios). In contrast to the work of Yang et al. where the pulse duration was 10 ns, under these conditions the charge carrier generation rate under illumination will be in equilibrium over the pulse duration (which is much longer than the typical charge carrier recombination lifetimes) and independent of the modulation frequency. As shown in Figure 4 (and for further frequencies in Figure S19 in the SI), no change in segregation dynamics beyond minor random variations is observed when the frequency is varied over 2.5 orders of magnitude from 10 to 3500 Hz, thus proving that the pulse frequency of the illumination alone does not directly affect halide segregation.

Given the similarity in perovskite composition between our work and that of Yang et al.,[46] we are further able to show that the observation of an apparent change in segregation dynamics with pulse repetition rate is fully compatible with the empirical
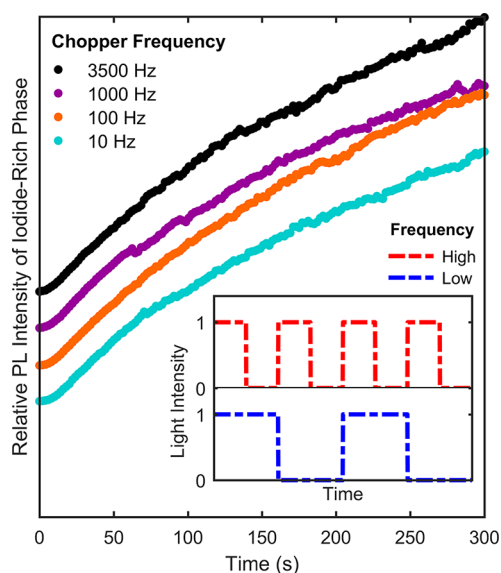
Figure 4. Increase in iodide-rich perovskite PL (integrated from 720 to 770 nm and normalized to the initial mixed-phase perovskite PL taken from 640 to 690 nm) as a $MAPb(Br_{0.5}I_{0.5})_3$ film is subjected to illumination through a chopper blade rotating at various frequencies. Curves start at zero and have been offset for clarity. The similar signal growth observed irrespective of chopper frequency shows that illumination pulse frequency has no direct effect on the halide segregation dynamics. Curves taken at additional frequencies are shown in Figure S19 in the SI.

model captured by eq 1. Using information provided in ref 46, we are able to evaluate the fractions of charge carriers recombining through traps and the number of incident photons per unit volume for the data taken by Yang et al. at different pulse repetition rates (see section S7 in the SI for full details). The squares shown in Figure 3 are then placed at the corresponding points on the graph, with the interior color of the squares indicating the corresponding level of low-bandgap PL growth reported by Yang et al. according to the scale on the right. Comparison of colors inside of the squares with the surrounding color of the false-color plot given by eq 1 thus allows for quantitative comparison of our empirical model against the outcome of their work. We note an excellent match between the two, in particular, the 2 kHz data point (yellow interior color) is indeed predicted and observed to fall where the iodide-rich perovskite emission begins to dominate the PL spectrum. Therefore, the apparent decrease in halide segregation with decreased pulse repetition rate in the experiments conducted by Yang et al. is solely related to the concomitant increase in initially injected charge carriers, which means that a larger fraction of charges will recombine through radiative band-to-band recombination, and consequently, fewer will be trapped.

From our empirical model of halide segregation, we are also able to determine the trap-mediated charge carrier recombination rate for which $MAPb(Br_{0.5}I_{0.5})_3$ perovskite would be sufficiently stable against segregation over the course of 1 day under 1 sun illumination. Such calculations are valuable as they can serve as guidance to materials design and set an outlook to what must be achieved in order to make perovskite−silicon tandem cells viable. The detrimental effect of halide segregation on PV device performance has recently been reported;[14−16] however, Duong et al. also showed experimentally that such effects were less severe for

$Rb_{0.05}(Cs_{0.1}MA_{0.15}FA_{0.75})_{0.95}Pb(Br_{0.33}I_{0.67})_3$ (FA = CH-$(NH_2)_2^+$) perovskite devices under illumination when the films were operated at maximum power point or short-circuit conditions, rather than at open-circuit.[16] These observations can be fully understood within our empirical model because charge carrier extraction—a process inherent in electricity generation—provides a competing process to that of charge carrier recombination, thus lowering the fraction of charge carriers that are trapped and therefore stabilizing the film against halide segregation. To account for such charge carrier extraction here, we use a simple approximation to integrate an extraction rate into the standard, third-order charge carrier recombination rate equation, as proposed by Lin et al.[52]

$$\frac{dn}{dt} = G - k_1 n - k_2 n^2 - k_3 n^3 - c_{ext} n \tag{2}$$

Here, n is the charge carrier density, t is time, G is the generation rate, k_1, k_2, and k_3 are the trap-mediated (monomolecular), band-to-band (bimolecular), and Auger recombination rate constants, respectively, and c_{ext} is the charge carrier extraction rate.

To determine the value of k_1 required to limit halide segregation, we first evaluate the borderline value of g for which $I_{(I\text{-rich PL})} = 1$ in eq 1, i.e., our condition of stability against halide segregation is that the PL originating from the iodide-rich phase must remain equal or smaller than the initial mixed-phase PL peak intensity. Solving eq 1 for this case while taking the generation rate, G, under solar illumination (see SI section S3), a time, t, of 12 h, and the fitting parameters A and B determined above to be 43.6 and 27.5×10^{-3} allows us to determine the value of the scaling factor, g, which will prevent significant segregation under these conditions to be 1.01×10^{-26} cm³. Extrapolating the linear fit presented in Figure 2b to this value of g then determines that the fraction of charge carriers that recombine through trap states must be lower than about 0.1% for significant segregation to be avoided in $MAPb(Br_{0.5}I_{0.5})_3$ films under solar illumination. Finally, under continuous illumination, eq 2 will be equal to zero, which allows us to determine the required value of k_1 given G, k_2, k_3, c_{ext}, and the condition that the fraction of charge carriers that recombine through trap states, $\frac{k_1 n}{G}$, is equal to 0.1%. For this purpose, we again use our calculated value of G under solar illumination (see SI section S3), assume k_2 to be 6×10^{-10} cm³ s⁻¹ as determined from our samples (see SI section S8) and k_3 to be 10^{-28} cm⁶ s⁻¹ in accordance with similar perovskites,[51] and take a typical value of c_{ext} to be 10^8 s⁻¹ as suggested by Lin et al.[52] From such considerations, we calculate a value for k_1 of 10^5 s⁻¹ (corresponding to a PL lifetime of $\tau_{PL} = (2k_1)^{-1} = 5$ μs at low excitation fluence) to be just sufficient to prevent the iodide-rich perovskite PL peak from becoming dominant in the PL spectrum of $MAPb(Br_{0.5}I_{0.5})_3$ over the course of 0.5 days of full solar illumination (see SI section S9 for a more detailed discussion of the calculation presented here).

We note that values of k_1 near $\sim10^5$ s⁻¹ have been achieved for other perovskites,[53] and hence it is not unfeasible that $MAPb(Br_{0.5}I_{0.5})_3$ could reach these with further advances in processing and defect passivation. In addition, mixed-halide perovskites other than $MAPb(Br_{0.5}I_{0.5})_3$ may be associated with a different set of parameters A, B, and g, which yield potentially less stringent requirements for lowering trap-related charge carrier recombination. We note that the $Cs_yFA_{(1-y)}Pb$-$(Br_xI_{(1-x)})_3$ system has shown much lower propensity for

halide segregation in the critical region ($0.3 < x < 0.5$) than the corresponding MA-based perovskites[17] provided the Cs fraction is within the range of ~10–30%. This system also exhibits clear correlations between trap-mediated recombination rates and propensity for halide segregation[17] but appears to achieve stability at higher values of k_1 than those we predict to be required for $MAPb(Br_{0.5}I_{0.5})_3$. Therefore, with both stoichiometric and structural engineering, as well as lowering of defect concentrations, it should be possible to suppress halide segregation sufficiently in functional perovskite solar cells.

The results presented here on the role of electronic trap states in halide segregation allow us to propose the following description of the underlying mechanisms. Prior to illumination, iodide and bromide ions are entropically well mixed in the perovskite, which therefore has a constant bandgap across all regions of the film. Although the nature of trap states is not yet entirely understood in hybrid perovskite materials,[54,55] reports have suggested that electrons are more likely to be trapped than holes[56,57] and that these trapped carriers are very long lived (on the order of tens of microseconds).[57,58] Initially upon illumination, any trapped electrons will electrostatically attract the photogenerated free holes, reducing the distance between the two and therefore minimizing the electric potential in the perovskite film. Additionally, random thermal movements of the halide ions and free charge carriers may eventually cause small regions of iodide-rich perovskite to form. With a higher valence band,[40,59] these regions act to draw free holes away from the trapped electrons states, creating a degree of charge separation between the randomly distributed trap states and the iodide-rich regions of perovskite, which thus establishes an electric field in the film. This field increases the degree of halide segregation, which increases the degree of charge separation, thus increasing the strength of the electric field in a feedback loop. Eventually the perovskite film is maximally segregated and limited by back-diffusion of the halide ions due to the large concentration gradient, i.e., the film reaches equilibrium. Without illumination and once the trapped charge carriers have recombined, the created electric field vanishes and the halide ions diffuse and remix. This description explains various observed phenomena, including that charge carriers,[14,16] electronic trap states, and film crystallinity[17–19] all influence halide segregation and the initially slow, asymptotic evolution (Figure S14 and S15) of the iodide-rich perovskite PL intensity reported in this work.

In summary, we demonstrated that the environmental atmosphere has a profound impact on the halide segregation dynamics in $MAPb(Br_{0.5}I_{0.5})_3$ observed through PL experiments under illumination. In particular, repeated cycles of illumination followed by darkness did not yield identical results when the perovskite was held in air or vacuum, most likely because these environments induce trap passivation or formation, respectively, in analogy to what had previously been reported for single-halide perovskites[20,22,24,26,28] On the other hand, halide segregation was found to be mostly reversible under inert nitrogen or when the film was encapsulated with a PMMA coating. We conclude that in fully encapsulated photovoltaic devices, halide segregation should therefore be a fully reversible process. Our findings further highlight a potential source for the discrepancies between different reports of halide segregation in the literature, which may partly derive from experiments having been conducted in a variety of atmospheres. We suggest that coating samples with PMMA prior to investigation and careful

recording of environmental parameters would be helpful for future experiments.

In addition, we explored the influence of trap states on the rate of halide segregation by monitoring the segregation dynamics for different charge carrier densities. We showed that the formation dynamics of iodide-rich emission from the perovskite film follows the same functional form, regardless of illumination conditions. We further established that the efficacy of a photon to induce halide segregation is higher the lower the charge carrier density, which we attribute to the larger relative fraction of charge carriers being trapped at these low densities. From these observations, we were able to establish an empirical model that directly links the amount of halide segregation observed in PL to the fraction of charge carriers recombining through trap-mediated channels and the photon flux absorbed. Such quantitative analysis allowed us to draw a number of conclusions on open questions on the mechanism driving halide segregation. For example, we were able to reveal that if modulated light is used to photoexcite mixed-halide perovskites, the frequency of the modulation alone has no influence on the segregation dynamics. In addition, we extrapolated that working perovskite solar cells based on $MAPb(Br_{0.5}I_{0.5})_3$ would require a reduction of the trap-related charge carrier recombination rate to $\lesssim 10^5$ s^{-1} ($\tau_{PL} \gtrsim 5$ μs) in order for halide segregation to be sufficiently suppressed. Our results suggest that light-induced halide segregation is initiated by electric fields arising from trapped charge carriers and may be further driven by funneling of charge carriers into the newly formed lower-energy iodide-rich domains. These findings contribute to our understanding of the mysterious underlying mechanics of halide ion movement in perovskites and provide a framework for determining the conditions required for stabilized perovskite devices under working conditions.

■ ASSOCIATED CONTENT

ⓢ Supporting Information

The Supporting Information is available free of charge on the ACS Publications website at DOI: 10.1021/acsenergylett.8b02002.

> Sample fabrication method, sample characterization (SEM, XRD, absorption spectrum), calculations of AM1.5 equivalent intensity, individual segregation measurements under different atmospheres, further discussion of segregation experiments under constant photon exposure, discussion of charge carrier dynamics, discussion of the dependence of halide segregation on pulse frequency, time-correlated single-photon counting measurements, and calculations of stability conditions under real-world conditions (PDF)

■ AUTHOR INFORMATION

Corresponding Author

*E-mail: laura.herz@physics.ox.ac.uk.

ORCID Ⓞ

Henry J. Snaith: 0000-0001-8511-790X

Michael B. Johnston: 0000-0002-0301-8033

Laura M. Herz: 0000-0001-9621-334X

Notes

The authors declare no competing financial interest.

■ REFERENCES

(1) Ono, L. K.; Park, N.-G.; Zhu, K.; Huang, W.; Qi, Y. Perovskite Solar Cells Towards Commercialization. *ACS Energy Lett.* **2017**, 2, 1749−1751.

(2) Berry, J. J.; van de Lagemaat, J.; Al-Jassim, M. M.; Kurtz, S.; Yan, Y.; Zhu, K. Perovskite Photovoltaics: The Path to a Printable Terawatt-Scale Technology. *ACS Energy Lett.* **2017**, 2, 2540−2544.

(3) Green, M. A. Commercial Progress and Challenges for Photovoltaics. *Nat. Energy* **2016**, 1, 15015.

(4) McMeekin, D. P.; Sadoughi, G.; Rehman, W.; Eperon, G. E.; Saliba, M.; Hörantner, M. T.; Haghighirad, A.; Sakai, N.; Korte, L.; Rech, B.; et al. A Mixed-Cation Lead Mixed-Halide Perovskite Absorber for Tandem Solar Cells. *Science* **2016**, 351, 151−155.

(5) Albrecht, S.; Saliba, M.; Correa Baena, J. P.; Lang, F.; Kegelmann, L.; Mews, M.; Steier, L.; Abate, A.; Rappich, J.; Korte, L.; et al. Monolithic Perovskite/Silicon-Heterojunction Tandem Solar Cells Processed at Low Temperature. *Energy Environ. Sci.* **2016**, 9, 81−88.

(6) Bush, K. A.; Palmstrom, A. F.; Yu, Z. J.; Boccard, M.; Cheacharoen, R.; Mailoa, J. P.; McMeekin, D. P.; Hoye, R. L.; Bailie, C. D.; Leijtens, T.; et al. 23.6%-Efficient Monolithic Perovskite/Silicon Tandem Solar Cells with Improved Stability. *Nat. Energy* **2017**, 2, 17009.

(7) Werner, J.; Weng, C.-H.; Walter, A.; Fesquet, L.; Seif, J. P.; De Wolf, S.; Niesen, B.; Ballif, C. Efficient Monolithic Perovskite/Silicon Tandem Solar Cell with Cell Area > 1 cm.^{2}. *J. Phys. Chem. Lett.* **2016**, 7, 161−166.

(8) Shockley, W.; Queisser, H. J. Detailed Balance Limit of Efficiency of p-n Junction Solar Cells. *J. Appl. Phys.* **1961**, 32, 510−519.

(9) Noh, J. H.; Im, S. H.; Heo, J. H.; Mandal, T. N.; Seok, S. I. Chemical Management for Colorful, Efficient, and Stable Inorganic−Organic Hybrid Nanostructured Solar Cells. *Nano Lett.* **2013**, 13, 1764−1769.

(10) Unger, E.; Kegelmann, L.; Suchan, K.; Sörell, D.; Korte, L.; Albrecht, S. Roadmap and Roadblocks for the Band Gap Tunability of Metal Halide Perovskites. *J. Mater. Chem. A* **2017**, 5, 11401−11409.

(11) Jesper Jacobsson, T.; Correa-Baena, J.-P.; Pazoki, M.; Saliba, M.; Schenk, K.; Grätzel, M.; Hagfeldt, A. Exploration of the Compositional Space for Mixed Lead Halogen Perovskites for High Efficiency Solar Cells. *Energy Environ. Sci.* **2016**, 9, 1706−1724.

(12) Beal, R. E.; Slotcavage, D. J.; Leijtens, T.; Bowring, A. R.; Belisle, R. A.; Nguyen, W. H.; Burkhard, G. F.; Hoke, E. T.; McGehee, M. D. Cesium Lead Halide Perovskites with Improved Stability for Tandem Solar Cells. *J. Phys. Chem. Lett.* **2016**, 7, 746−751.

(13) Hoke, E. T.; Slotcavage, D. J.; Dohner, E. R.; Bowring, A. R.; Karunadasa, H. I.; McGehee, M. D. Reversible Photo-Induced Trap Formation in Mixed-Halide Hybrid Perovskites for Photovoltaics. *Chem. Sci.* **2015**, 6, 613−617.

(14) Braly, I. L.; Stoddard, R. J.; Rajagopal, A.; Uhl, A. R.; Katahara, J. K.; Jen, A. K.-Y.; Hillhouse, H. W. Current-Induced Phase Segregation in Mixed Halide Hybrid Perovskites and its Impact on Two-Terminal Tandem Solar Cell Design. *ACS Energy Lett.* **2017**, 2, 1841−1847.

(15) Samu, G. F.; Janáky, C.; Kamat, P. V. A Victim of Halide Ion Segregation. How Light Soaking Affects Solar Cell Performance of Mixed Halide Lead Perovskites. *ACS Energy Lett.* **2017**, 2, 1860−1861.

(16) Duong, T.; Mulmudi, H. K.; Wu, Y.; Fu, X.; Shen, H.; Peng, J.; Wu, N.; Nguyen, H. T.; Macdonald, D.; Lockrey, M.; et al. Light and Electrically Induced Phase Segregation and Its Impact on the Stability of Quadruple Cation High Bandgap Perovskite Solar Cells. *ACS Appl. Mater. Interfaces* **2017**, 9, 26859−26866.

(17) Rehman, W.; McMeekin, D. P.; Patel, J. B.; Milot, R. L.; Johnston, M. B.; Snaith, H. J.; Herz, L. M. Photovoltaic Mixed-Cation Lead Mixed-Halide Perovskites: Links Between Crystallinity, Photo-Stability and Electronic Properties. *Energy Environ. Sci.* **2017**, 10, 361−369.

(18) Hu, M.; Bi, C.; Yuan, Y.; Bai, Y.; Huang, J. Stabilized Wide Bandgap MAPbBr$_x$I$_{3−x}$ Perovskite by Enhanced Grain Size and Improved Crystallinity. *Adv. Sci.* **2016**, 3, 1500301.

(19) Zhou, Y.; Jia, Y.-H.; Fang, H.-H.; Loi, M. A.; Xie, F.-Y.; Gong, L.; Qin, M.-C.; Lu, X.-H.; Wong, C.-P.; Zhao, N. Composition-Tuned Wide Bandgap Perovskites: From Grain Engineering to Stability and Performance Improvement. *Adv. Funct. Mater.* **2018**, 28, 1803130.

(20) Brenes, R.; Eames, C.; Bulović, V.; Islam, M. S.; Stranks, S. D. The Impact of Atmosphere on the Local Luminescence Properties of Metal Halide Perovskite Grains. *Adv. Mater.* **2018**, 30, 1706208.

(21) Tian, Y.; Peter, M.; Unger, E.; Abdellah, M.; Zheng, K.; Pullerits, T.; Yartsev, A.; Sundström, V.; Scheblykin, I. G. Mechanistic Insights into Perovskite Photoluminescence Enhancement: Light Curing with Oxygen can Boost Yield Thousandfold. *Phys. Chem. Chem. Phys.* **2015**, 17, 24978−24987.

(22) Feng, X.; Su, H.; Wu, Y.; Wu, H.; Xie, J.; Liu, X.; Fan, J.; Dai, J.; He, Z. Photon-Generated Carriers Excite Superoxide Species Inducing Long-Term Photoluminescence Enhancement of MAPbI$_3$ Perovskite Single Crystals. *J. Mater. Chem. A* **2017**, 5, 12048−12053.

(23) Galisteo-Lopez, J. F.; Anaya, M.; Calvo, M.; Míguez, H. Environmental Effects on the Photophysics of Organic−Inorganic Halide Perovskites. *J. Phys. Chem. Lett.* **2015**, 6, 2200−2205.

(24) Brenes, R.; Guo, D.; Osherov, A.; Noel, N. K.; Eames, C.; Hutter, E. M.; Pathak, S. K.; Niroui, F.; Friend, R. H.; Islam, M. S.; et al. Metal Halide Perovskite Polycrystalline Films Exhibiting Properties of Single Crystals. *Joule* **2017**, 1, 155−167.

(25) Quitsch, W.-A.; deQuilettes, D. W.; Pfingsten, O.; Schmitz, A.; Ognjanovic, S. M.; Jariwala, S.; Koch, S.; Winterer, M.; Ginger, D. S.; Bacher, G. The Role of Excitation Energy in Photobrightening and Photodegradation of Halide Perovskite Thin Films. *J. Phys. Chem. Lett.* **2018**, 9, 2062−2069.

(26) Kheraj, V.; Simonds, B. J.; Toshniwal, A.; Misra, S.; Peroncik, P.; Zhang, C.; Vardeny, Z.; Scarpulla, M. A. Using Photoluminescence to Monitor the Optoelectronic Properties of Methylammonium Lead Halide Perovskites in Light and Dark over Periods of Days. *J. Lumin.* **2018**, 194, 353−358.

(27) Fang, H.-H.; Adjokatse, S.; Wei, H.; Yang, J.; Blake, G. R.; Huang, J.; Even, J.; Loi, M. A. Ultrahigh Sensitivity of Methylammonium Lead Tribromide Perovskite Single Crystals to Environmental Gases. *Sci. Adv.* **2016**, 2, No. e1600534.

(28) Motti, S. G.; Gandini, M.; Barker, A. J.; Ball, J. M.; Srimath Kandada, A. R.; Petrozza, A. Photoinduced Emissive Trap States in Lead Halide Perovskite Semiconductors. *ACS Energy Lett.* **2016**, 1, 726−730.

(29) Aristidou, N.; Sanchez-Molina, I.; Chotchuangchutchaval, T.; Brown, M.; Martinez, L.; Rath, T.; Haque, S. A. The Role of Oxygen in the Degradation of Methylammonium Lead Trihalide Perovskite Photoactive Layers. *Angew. Chem., Int. Ed.* **2015**, 54, 8208−8212.

(30) Aristidou, N.; Eames, C.; Sanchez-Molina, I; Bu, X.; Kosco, J.; Islam, M. S.; Haque, S. A. Fast Oxygen Diffusion and Iodide Defects Mediate Oxygen-Induced Degradation of Perovskite Solar Cells. *Nat. Commun.* **2017**, 8, 15218.

(31) Yang, J.; Siempelkamp, B. D.; Liu, D.; Kelly, T. L. Investigation of CH$_3$NH$_3$PbI$_3$ Degradation Rates and Mechanisms in Controlled Humidity Environments Using In Situ Techniques. *ACS Nano* **2015**, 9, 1955−1963.

(32) Tong, C.-J.; Geng, W.; Tang, Z.-K.; Yam, C.-Y.; Fan, X.-L.; Liu, J.; Lau, W.-M.; Liu, L.-M. Uncovering the Veil of the Degradation in Perovskite CH$_3$NH$_3$PbI$_3$ upon Humidity Exposure: a First-Principles Study. *J. Phys. Chem. Lett.* **2015**, 6, 3289−3295.

(33) Anizelli, H. S.; Fernandes, R. V.; Scarmínio, J.; da Silva, P. R. C.; Duarte, J. L.; Laureto, E. Effect of Pressure on the Remixing

Process in CH₃NH₃Pb(I₁₋ₓBrₓ)₃ Perovskite Thin Films. *J. Lumin.* **2018**, *199*, 348−351.

(34) Chen, Q.; Zhou, H.; Song, T.-B.; Luo, S.; Hong, Z.; Duan, H.-S.; Dou, L.; Liu, Y.; Yang, Y. Controllable Self-Induced Passivation of Hybrid Lead Iodide Perovskites Toward High Performance Solar Cells. *Nano Lett.* **2014**, *14*, 4158−4163.

(35) Eames, C.; Frost, J. M.; Barnes, P. R.; O'Regan, B. C.; Walsh, A.; Islam, M. S. Ionic Transport in Hybrid Lead Iodide Perovskite Solar Cells. *Nat. Commun.* **2015**, *6*, 7497.

(36) Yang, B.; Brown, C. C.; Huang, J.; Collins, L.; Sang, X.; Unocic, R. R.; Jesse, S.; Kalinin, S. V.; Belianinov, A.; Jakowski, J.; et al. Enhancing Ion Migration in Grain Boundaries of Hybrid Organic−Inorganic Perovskites by Chlorine. *Adv. Funct. Mater.* **2017**, *27*, 1700749.

(37) Shao, Y.; Fang, Y.; Li, T.; Wang, Q.; Dong, Q.; Deng, Y.; Yuan, Y.; Wei, H.; Wang, M.; Gruverman, A.; et al. Grain Boundary Dominated Ion Migration in Polycrystalline Organic−Inorganic Halide Perovskite Films. *Energy Environ. Sci.* **2016**, *9*, 1752−1759.

(38) Yun, J. S.; Seidel, J.; Kim, J.; Soufiani, A. M.; Huang, S.; Lau, J.; Jeon, N. J.; Seok, S. I.; Green, M. A.; Ho-Baillie, A. Critical Role of Grain Boundaries for Ion Migration in Formamidinium and Methylammonium Lead Halide Perovskite Solar Cells. *Adv. Energy Mater.* **2016**, *6*, 1600330.

(39) Draguta, S.; Sharia, O.; Yoon, S. J.; Brennan, M. C.; Morozov, Y. V.; Manser, J. M.; Kamat, P. V.; Schneider, W. F.; Kuno, M. Rationalizing the Light-Induced Phase Separation of Mixed Halide Organic−Inorganic Perovskites. *Nat. Commun.* **2017**, *8*, 200.

(40) Yoon, S. J.; Draguta, S.; Manser, J. S.; Sharia, O.; Schneider, W. F.; Kuno, M.; Kamat, P. V. Tracking Iodide and Bromide Ion Segregation in Mixed Halide Lead Perovskites During Photo-irradiation. *ACS Energy Lett.* **2016**, *1*, 290−296.

(41) Slotcavage, D. J.; Karunadasa, H. I.; McGehee, M. D. Light-Induced Phase Segregation in Halide-Perovskite Absorbers. *ACS Energy Lett.* **2016**, *1*, 1199−1205.

(42) Yoon, S. J.; Kuno, M.; Kamat, P. V. Shift Happens. How Halide Ion Defects Influence Photoinduced Segregation in Mixed Halide Perovskites. *ACS Energy Lett.* **2017**, *2*, 1507−1514.

(43) Barker, A. J.; Sadhanala, A.; Deschler, F.; Gandini, M.; Senanayak, S. P.; Pearce, P. M.; Mosconi, E.; Pearson, A. J.; Wu, Y.; Srimath Kandada, A. R.; et al. Defect-Assisted Photoinduced Halide Segregation in Mixed-Halide Perovskite Thin Films. *ACS Energy Lett.* **2017**, *2*, 1416−1424.

(44) Rehman, W.; Milot, R. L.; Eperon, G. E.; Wehrenfennig, C.; Boland, J. L.; Snaith, H. J.; Johnston, M. B.; Herz, L. M. Charge-Carrier Dynamics and Mobilities in Formamidinium Lead Mixed-Halide Perovskites. *Adv. Mater.* **2015**, *27*, 7938−7944.

(45) Bischak, C. G.; Hetherington, C. L.; Wu, H.; Aloni, S.; Ogletree, D. F.; Limmer, D. T.; Ginsberg, N. S. Origin of Reversible Photoinduced Phase Separation in Hybrid Perovskites. *Nano Lett.* **2017**, *17*, 1028−1033.

(46) Yang, X.; Yan, X.; Wang, W.; Zhu, X.; Li, H.; Ma, W.; Sheng, C. Light Induced Metastable Modification of Optical Properties in CH₃NH₃PbI₃₋ₓBrₓ Perovskite Films: Two-Step Mechanism. *Org. Electron.* **2016**, *34*, 79−83.

(47) Brennan, M. C.; Draguta, S.; Kamat, P. V.; Kuno, M. Light-Induced Anion Phase Segregation in Mixed Halide Perovskites. *ACS Energy Lett.* **2018**, *3*, 204−213.

(48) Brivio, F.; Caetano, C.; Walsh, A. Thermodynamic Origin of Photoinstability in the CH₃NH₃Pb(I₁₋ₓBrₓ)₃ Hybrid Halide Perovskite Alloy. *J. Phys. Chem. Lett.* **2016**, *7*, 1083−1087.

(49) Tang, X.; van den Berg, M.; Gu, E.; Horneber, A.; Matt, G. J.; Osvet, A.; Meixner, A. J.; Zhang, D.; Brabec, C. J. Local Observation of Phase Segregation in Mixed-Halide Perovskite. *Nano Lett.* **2018**, *18*, 2172−2178.

(50) Li, W.; Rothmann, M. U.; Liu, A.; Wang, Z.; Zhang, Y.; Pascoe, A. R.; Lu, J.; Jiang, L.; Chen, Y.; Huang, F.; et al. Phase Segregation Enhanced Ion Movement in Efficient Inorganic CsPbIBr₂ Solar Cells. *Adv. Energy Mater.* **2017**, *7*, 1700946.

(51) Johnston, M. B.; Herz, L. M. Hybrid Perovskites for Photovoltaics: Charge-Carrier Recombination, Diffusion, and Radiative Efficiencies. *Acc. Chem. Res.* **2016**, *49*, 146−154.

(52) Lin, Q.; Wang, Z.; Snaith, H. J.; Johnston, M. B.; Herz, L. M. Hybrid Perovskites: Prospects for Concentrator Solar Cells. *Adv. Sci.* **2018**, *5*, 1700792.

(53) deQuilettes, D. W.; Koch, S.; Burke, S.; Paranji, R. K.; Shropshire, A. J.; Ziffer, M. E.; Ginger, D. S. Photoluminescence Lifetimes Exceeding 8 μs and Quantum Yields Exceeding 30% in Hybrid Perovskite Thin Films by Ligand Passivation. *ACS Energy Lett.* **2016**, *1*, 438−444.

(54) Ball, J. M.; Petrozza, A. Defects in Perovskite-Halides and Their Effects in Solar Cells. *Nat. Energy* **2016**, *1*, 16149.

(55) Stranks, S. D. Nonradiative Losses in Metal Halide Perovskites. *ACS Energy Lett.* **2017**, *2*, 1515−1525.

(56) Wetzelaer, G.-J. A.; Scheepers, M.; Sempere, A. M.; Momblona, C.; Avila, J.; Bolink, H. J. Trap-Assisted Non-Radiative Recombination in Organic−Inorganic Perovskite Solar Cells. *Adv. Mater.* **2015**, *27*, 1837−1841.

(57) Leijtens, T.; Eperon, G. E.; Barker, A. J.; Grancini, G.; Zhang, W.; Ball, J. M.; Kandada, A. R. S.; Snaith, H. J.; Petrozza, A. Carrier Trapping and Recombination: the Role of Defect Physics in Enhancing the Open Circuit Voltage of Metal Halide Perovskite Solar Cells. *Energy Environ. Sci.* **2016**, *9*, 3472−3481.

(58) Stranks, S. D.; Burlakov, V. M.; Leijtens, T.; Ball, J. M.; Goriely, A.; Snaith, H. J. Recombination Kinetics in Organic-Inorganic Perovskites: Excitons, Free Charge, and Subgap States. *Phys. Rev. Appl.* **2014**, *2*, 034007.

(59) Schulz, P.; Edri, E.; Kirmayer, S.; Hodes, G.; Cahen, D.; Kahn, A. Interface Energetics in Organo-Metal Halide Perovskite-Based Photovoltaic Cells. *Energy Environ. Sci.* **2014**, *7*, 1377−1381.